SLAC-PUB-1045
April 1972

CROSS-OVER EFFECT IN INELASTIC REACTIONS*

D. W. G. S. LEITH

INTRODUCTION

Let me quickly remind you of the application of the idea of duality to studies of production mechanism and dynamics in two and quasi-two body reactions. We used to think in terms of two separate energy regions -- low and high energy -- which were dominated by different processes -- resonance formation and exchange processes -- (See Fig. 1) and characterised by very different structure in energy, s, and in momentum transfer, t. The concept of duality implies an equivalence of these two pictures and the Finite Energy Sum Rules, FESR's provide the formal connection between them.

Two Component Duality asserts that the duality relations between the high energy region and the low energy region are satisfied between quite specific contributions to the whole scattering amplitude. More particularly, the low energy region may be thought of as being built from resonances and a background which lies below the peaks, while the high energy region is thought to be built from

* Work supported by the U.S. Atomic Energy Commission.
(Presented at the 7th Recontre de Moriond, Meribel-les-Allues, France, March 5-17, 1972)

various types of exchange process, divided into Pomeron exchanges and Regge exchanges. Two Component Duality would then imply that the resonance contributions are dual to Regge exchanges and that the background below the resonances is dual to the Pomeron exchange at high energy.

Further it is supposed that the Regge exchanges would be dominated by the larger impact parameter, and be quite peripheral in nature. By contrast, the Pomeron exchange is expected to have contributions from all partial waves.

These ideas are more completely discussed and nicely explained in several good reviews,[1] and also elegantly confirmed in a beautiful CERN-Orsay experiment studying elastic scattering at 5 GeV/c. The preliminary results showing cross-over in the K^+p and $p^{\mp}p$ elastic differential cross sections were presented at this meeting[2] last year, and the final data have just been published.[3] The same qualitative effects are observed in the preliminary data from ANL presented at this meeting.[4] Davier and Harari[5] have analysed the 5 GeV/c data and shown that indeed the Regge amplitude is peripheral, and that the Pomeron term has contributions from all partial waves. See Figs. 2 and 3.

The isolation of the imaginary part of the Regge amplitude is obtained from the following simple argument: They supposed that since the K^+p is exotic in the s-channel, that only the Pomeron contributes to that amplitude, but that for K^-p, both Pomeron and Regge contribute. Then they write

$$A(K^+p) = P$$

$$A(K^-p) = P + R$$

where P represents the Pomeron amplitude, purely imaginary, and R represents the complex Regge amplitude.

Then,

$$\text{Im } R = \frac{\frac{d\sigma}{dt}(K^-p) - \frac{d\sigma}{dt}(K^+p)}{2\sqrt{\frac{d\sigma}{dt}(K^+p)}}$$

$$= Ae^{bt} J_o(r\sqrt{-t}).$$

The data are well fit by this description, as shown in Fig. 4.

It is of interest to study this phenomenon in other diffractive processes.

THE $K_L^o p$ EXPERIMENT

At SLAC we have been studying the $K_L^o p$ interactions from (1-12) GeV/c in the 40" HBC. The work has been done by G. W. Brandenburg, W. B. Johnson, D. W. G. S. Leith, J. S. Loos, G. J. Luste, J. A. J. Matthews, K. Moriyasu, W. M. Smart, F. C. Winkelmann, and R. J. Yamartino. I wish to report some results on the inelastic diffractive processes

$$K^o p \to Q^o p \quad \text{and} \quad \bar{K}^o p \to \bar{Q}^o p.$$

The K_L^o beam is obtained when 19 GeV electrons are targetted on a one radiation length block of Be, and the resulting small angle K^o, (typically $1\text{-}1/2^o$), collimated, cleaned of photons and charged particles and let fly 55 meters to the HBC, by which time it is all K_L^o. The beam size at the bubble chamber is ~ (15 x 40) cms. We have scanned 800,000 pictures for 3 prong + V^o events, and obtained

a sample of 10,000 $K_1^o p\ \pi^+\pi^-$ events in the momentum region (1-12) GeV/c. The momentum spectrum of the beam is shown in Fig. 5, and represents an integrated path length of 32 events/μb. The absolute normalisation of the beam flux, and hence the cross sections is ~ 15%, but clearly relative K to $\bar{K}$ companions can be done with good accuracy, since the K_L^o beam has equal components of strangeness $\pm$ 1.

The cross section for the reaction is shown in Fig. 6 where the line represents a fall off in momentum of $p^{-1.6}$. The cross section for Q production is also shown in this figure, where the Q region is defined as:

(a) $1.1 \leq M\ (K\pi\pi) \leq 1.5$ GeV

(b) $t' < 0.5$ GeV^2

(c) $M(p\pi^+) > 1.3$ GeV

(d) $0.86 < M(K\pi) < 0.92$ -- double K* omitted.

The effect of cut (c) was evaluated using a Monte Carlo program and the corrections, as a function of momentum, applied to the cross section. The very tight selection of K*, gives a good signal to noise for this test, which is our handle on the strangeness of the Q (i.e. Q's decay into $K^{*+}\ \pi^-$, while $\bar{Q}$'s decay into $K^{*-}\pi^+$). The Q cross section is rather flat beyond 5 GeV/c, and falls like $p^{-0.59 \pm .16}$. This is to be compared to other processes:

$$\sigma \propto p^{-n}$$

$K^o p \rightarrow Q^o p$	$n = 0.59 \pm .16$
$K^+ p \rightarrow Q^+ p$	$= 0.58 \pm .15$
$\pi^- p \rightarrow A_1^- p$	$= 0.42 \pm .11$
$K^+ p \rightarrow K^+ p$	$= 0.09 \pm .03$
$K^- p \rightarrow K^- p$	$= 0.4 \pm .04$

It is also interesting to note the ratio of the s = +1 cross section to the s = -1 cross section, (see Fig. 7). The ratio is consistent with unity over the entire momentum region.

The reactions $K^o p \rightarrow Q^o p$ and $\overline{K}^o p \rightarrow \overline{Q}^o p$ are very similar in their cross section properties to the elastic scattering data. What about the differential cross section?

In Fig. 8 the differential cross section for the $K \rightarrow Q$ reactions are shown. The Q data, averaged over the momentum region (4-12) GeV/c shows a slope, $d\sigma/dt = Ae^{bt}$, of $b = 5.9 \pm .5$ GeV^2, while the $\overline{Q}$ data exhibits a much steeper slope of $b = 9.7 \pm .7$ GeV^2. In addition, the cross sections show a cross over at $t \sim 0.13$ GeV^2.

Indeed this inelastic process shows many of the same properties of the elastic reaction.

(The slope has been studied as a function of momentum and, despite being hampered by poor statistics, the same observation that $b^Q < b^{\overline{Q}}$ may be made, see Fig. 9.)

Having observed the cross-over effect, it is interesting to pursue the same analysis as has been discussed above for the elastic case. The diffraction dissociation of Q is, however, a more complicated reaction, having six independent amplitudes in place of the two for elastic scattering. Nevertheless, we can proceed by averaging over the allowed helicity amplitudes and obtaining an "average imaginary Regge amplitude."

If we denote the change in helicity at the baryon vertex by λ, and at the meson vertex by μ, then we may write

$$\frac{d\sigma}{dt'}\,(K^{o}p \rightarrow Q^{o}p) = \sum_{\lambda\mu}\left[\left|P^{\lambda\mu}\right|^{2} + 2P^{\lambda\mu}\,(\mathrm{Im}\,R_{T}^{\lambda\mu} + \mathrm{Im}\,R_{V}^{\lambda\mu})\right]$$

$$\frac{d\sigma}{dt'}\,(\bar{K}^{o}p \rightarrow \bar{Q}^{o}p) = \sum_{\lambda\mu}\left[\left|P^{\lambda\mu}\right|^{2} + 2P^{\lambda\mu}\,(\mathrm{Im}\,R_{T}^{\lambda\mu} - \mathrm{Im}\,R_{V}^{\lambda\mu})\right]$$

where the Pomeron amplitude, P, has been assumed to be purely imaginary, and R_T represents a combination of A_2 and f exchanges, and R_V represents a combination of ρ and ω exchanges. For the exotic $K^{o}p$ reaction the amplitude is limited by duality to be predominantly real, and therefore to a good approximation, we may equate $d\sigma/dt\,(K^{o}p)$ to P^{2}. To obtain an estimate of the Regge contribution, we define the average

$$\langle \mathrm{Im}\,R_{t'}\rangle \sim \frac{\sum_{\lambda\mu} 2P^{\lambda\mu}\,\mathrm{Im}\,R_{V}^{\lambda\mu}}{2\left[\sum_{\lambda\mu}\left|P^{\lambda\mu}\right|^{2}\right]^{1/2}}$$

$$\sim \frac{\frac{d\sigma}{dt}\,(\bar{Q}^{o}p) - \frac{d\sigma}{dt'}\,(Q^{o}p)}{2\left[\frac{d\sigma}{dt'}(Q^{o}p)\right]^{1/2}}$$

Thus the cross over of the $Q^{o}p$ and $\bar{Q}^{o}p$ differential cross sections corresponds to a zero in the Regge contribution, $\langle \mathrm{Im}\,R \rangle$.

Experimental values of $\langle \mathrm{Im}\,R_{t'}\rangle$ have been evaluated from the differential cross sections and are shown in Fig. 10. The solid curve is taken from the exponential fits to the differential cross sections shown in Fig. 8, giving

$$\langle \mathrm{Im}\,R_{t'}\rangle = \left(\frac{1.36\,\exp\,(9.7\,t') - 0.83\,\exp\,(5.9\,t')}{2\left[\,0.83\,\exp\,(5.9\,t')\,\right]^{2}}\right)$$

The geometrical picture used by Davier and Harari described above, also fits the data (in our t interval) equally well,

$$\langle \mathrm{Im}\, R_{t'} \rangle = 0.3 \exp(0.7t') J_0(6.5\sqrt{-t})$$

The larger radius found here, (1.3 f as opposed to the 0.9 f in elastic scattering), should not be taken too literally, since several helicity amplitudes probably make important contributions to $\langle \mathrm{Im}\, R \rangle$.

In addition, we can comment on the strength of the Pomeron and Regge contributions in Q production relative to elastic scattering.

For our average beam momentum of ~ 7 GeV/c, the differential cross section at t' = 0 for $K^o p \to Q^o p$ in 3.9 ± 0.8 mb/GeV^2, when corrections are made for all unobserved decay modes of the Q^o. The forward differential cross section for $K^+ p$ elastic scattering at 7 GeV/c is 20 ± 4 mb/GeV^2.[6] For t' = 0 a study of the Q^o decay density matrix elements indicate $\lambda = \mu = 0$. We then find

$$\left| \frac{P^{oo}(0)}{Ap\ (0)} \right| = \left[\frac{\frac{d\sigma}{dt'}(K^o p \to Q^o p)}{\frac{d\sigma}{dt}\ (K^+ p \to K^+ p)} \right]^{1/2}_{t'=0}$$

$$= 0.41 \pm 0.1$$

where Ap is the Pomeron contribution to elastic scattering.

Thus the Pomeron amplitude is roughly half as big for Q production as for Kp elastic scattering.

For the Regge contribution, we have

$$2\ \mathrm{Im}\, R_V^{oo}(0) \sim \left(\frac{\frac{d\sigma}{dt'}(\bar{Q}^o p) - \frac{d\sigma}{dt'}(Q^o p)}{2\left[\frac{d\sigma}{dt'}\ (Q^o p)\right]^{1/2}} \right)_{t'=0}$$

The corresponding Regge amplitude in $K^o p$ and $\bar{K}^o p$ elastic scattering can be determined directly from the inelastic reaction $K_L^o p \to K_S^o p$, where

$$A(K_L^o p \to K_S^o p) = \frac{1}{2}\left[A(K^o p) - A(\bar{K}^o p)\right]$$
$$= A_V$$

The ratio of real to imaginary parts of $A_V(0)$ is known be near to unity.(7)

Therefore, we have

$$\frac{d\sigma}{dt}(K_S^o p)_{t-0} \sim 2\left[\text{Im } A_V(0)\right]^2$$

The ratio of the Regge amplitudes is then:

$$\left|\frac{\text{Im } R_V^{oo}(0)}{\text{Im } A_V(0)}\right| \sim \left\{\frac{\frac{d\sigma}{dt}(\bar{Q}^o p) - \frac{d\sigma}{dt}(Q^o p)}{\left[8\frac{d\sigma}{dt}(Q^o p) \cdot \frac{d\sigma}{dt}(K_S^o p)\right]^{1/2}}\right\}$$

Correcting for the unobserved decay modes of the Q meson and using experimental values(7) for the forward cross section for $K_L^o p \to K_S^o p$, we find at 7 GeV/c

$$\left|\frac{\text{Im } R_V^{oo}(0)}{\text{Im } A_V(0)}\right| = 0.8 \pm 0.3.$$

Therefore, we find approximately equal Regge contributions are found for the Q meson production and for $K^o p$, $\bar{K}^o p$ elastic scattering.

Finally, we find that $\int dt \left|\langle \text{Im } R_{t'} \rangle\right|^2 \sim 30$ μb when corrections are made for all decay modes of the Q^o. Therefore we expect that Q production in charge or hypercharge exchange reactions will have cross sections of the order of 30 μb in the momentum range (5-10) GeV/c.

CONCLUSIONS

It is interesting to see the features of slowly varying cross section, equality of particle and antiparticle cross sections and the occurence of a crossover in the differential cross section for particle and antiparticle processes appearing in the inelastic Q production just as in the elastic scattering.

The analysis of the differential cross sections, following Davier and Harari, shows that these reactions thought to be dominated by Pomeron exchange, have also substantial Regge contribution.

It will be interesting to see similar data for the reactions $\pi^{\pm}p \rightarrow A_1^{\pm}p$ and $p^{\pm}p \rightarrow (p\pi\pi)^{\pm}\, p$.

REFERENCES

1. H. Harari, Brookhaven Summer School (1969); M. Kugler, Acta Physica Austriaca, Suppl. VII, 443 (1970); H. Harari, SLAC PUB-914.
2. C. Baglin, Proceedings of the 6th Rencontre de Moriond, (1971).
3. V. Chaband et al., CERN Preprint (submitted to Physics Letters).
4. A. Yokosawa, presented preliminary results of R. Diebold et al. on $\pi^{\pm}p$, $K^{\pm}p$, $p^{\pm}p$ elastic scattering at 3.6 GeV/c at this meeting.
5. M. Davier and H. Harari, Physics Letters 35B, 239 (1971).
6. K. Foley et al., Phys. Rev. Letters 11, 503 (1963).
7. A. D. Brody et al., Phys. Rev. Letters 26, 1050 (1971); C. D. Buchanan et al., Physics Letters 37B, 213 (1971); P. Darriulat et al., Physics Letters 33B, 433 (1970).

FIGURE CAPTIONS

Fig. 1 Schematic characteristics of the low and high energy scattering regions.

Fig. 2 Legendre coefficients a_J for the amplitude R(+)- the Regge contribution. (Taken from reference 5.)

Fig. 3 Legendre coefficients a_J for $P(+) = \sqrt{d\sigma/dt}(K^+p)$ (labelled K^+p) and for $P(t) + R(t) = \sqrt{d\sigma/dt}(K^-p)$ (labelled K^-p). (Taken from reference 5.)

Fig. 4 The experimental results for

$$\frac{\frac{d\sigma}{dt}(K^-p) - \frac{d\sigma}{dt}(K^+p)}{2\sqrt{\frac{d\sigma}{dt}(K^+p)}}$$

as a function of t. (Taken from reference 5.)

Fig. 5 The momentum spectrum of K_L^o at the 40" HBC.

Fig. 6 The cross section for the reaction $K_L^o p \rightarrow K_S^o p\pi^+\pi^-$ (ϕ), and for the quasi-two body sub-reaction $K_L^o p \rightarrow Qp$ ($\square$).

Fig. 7 The ratio of the cross sections for the reactions $K^o p \rightarrow Q^o p$ and $\bar{K}^o p \rightarrow \bar{Q}^o p$.

Fig. 8 The differential cross section for $\bar{K}^o p \rightarrow \bar{Q}^o p$ (ϕ), and for $K^o p \rightarrow Q^o p$ ($\blacksquare$). The lines are the results of exponential fits to the cross section, $d\sigma/dt = Ae^{bt}$.

Fig. 9 The slope of the differential cross sections for $\bar{K}^o p \rightarrow \bar{Q}^o p$ (ϕ), and $K^o p \rightarrow Q^o p$ ($\blacksquare$) as a function of beam momentum.

Fig. 10 The average $\langle \text{Im } R \rangle$ for the Q production process, isolated by taking

$$\langle \text{Im } R \rangle = \frac{\frac{d\sigma}{dt'}(\bar{Q}^{o}p) - \frac{d\sigma}{dt'}(Q^{o}p)}{2\left[\frac{d\sigma}{dt'}(Q^{o}p)\right]^{1/2}} .$$

The solid line comes from the exponential fits to the cross sections, while the darker line comes from the "J_o" form suggested by Davier and Harari. (See text.)

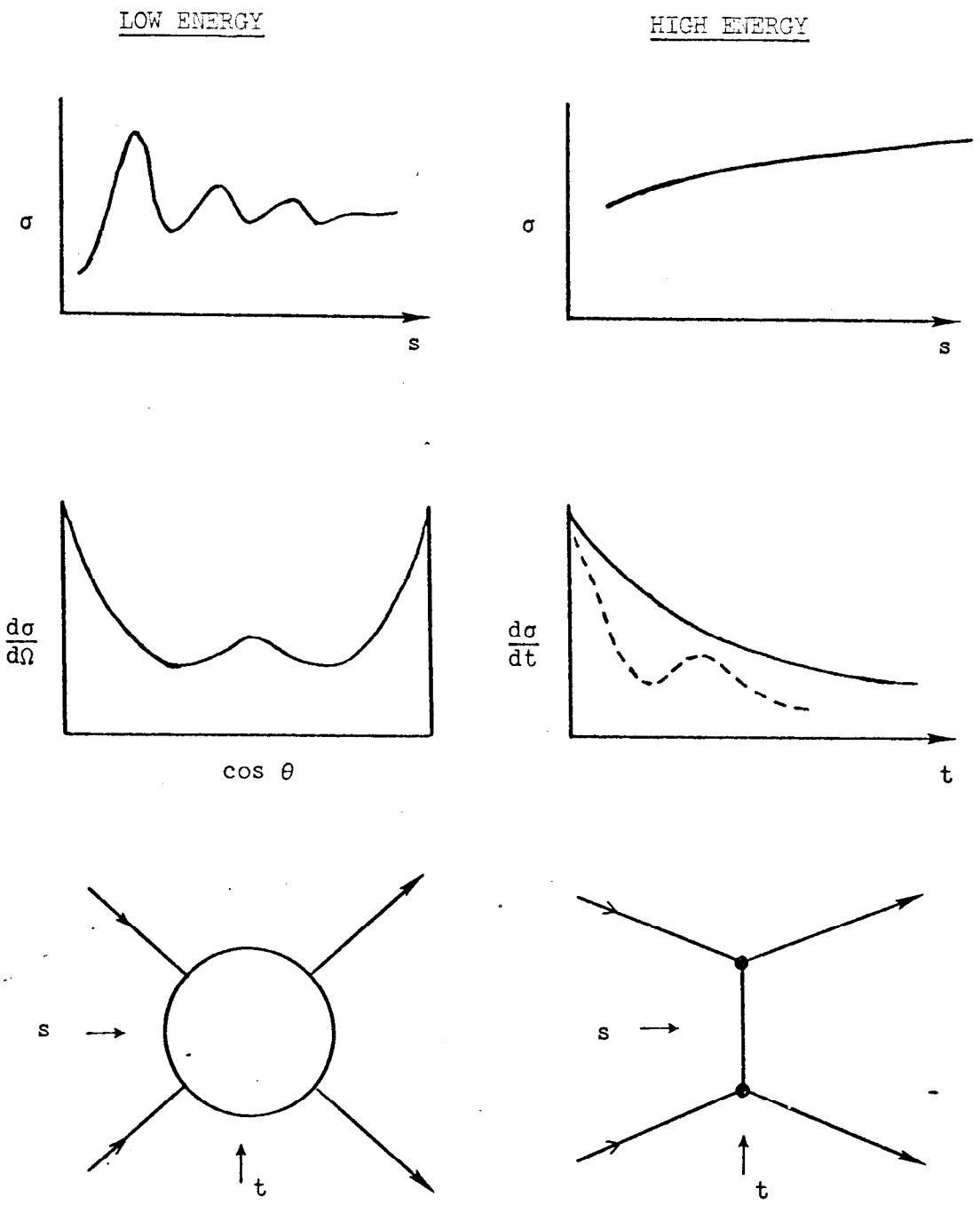

Fig. 1

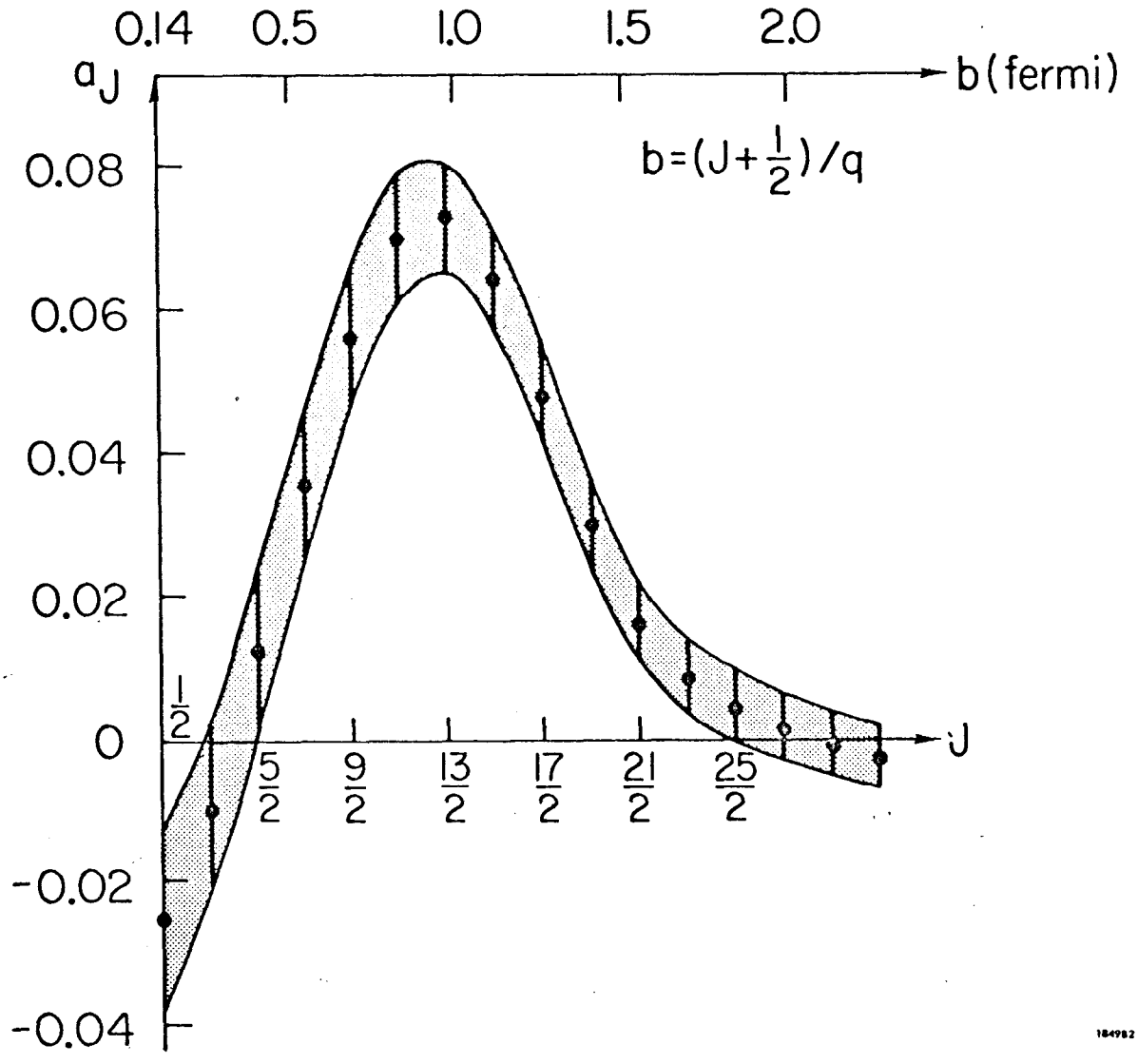
0.14
0.5
1.0
1.5
2.0
a_J
b(fermi)
$b=(J+\frac{1}{2})/q$
0.08
0.06
0.04
0.02
0
-0.02
-0.04
$\frac{1}{2}$
$\frac{5}{2}$
$\frac{9}{2}$
$\frac{13}{2}$
$\frac{17}{2}$
$\frac{21}{2}$
$\frac{25}{2}$
J
184982

Fig. 2

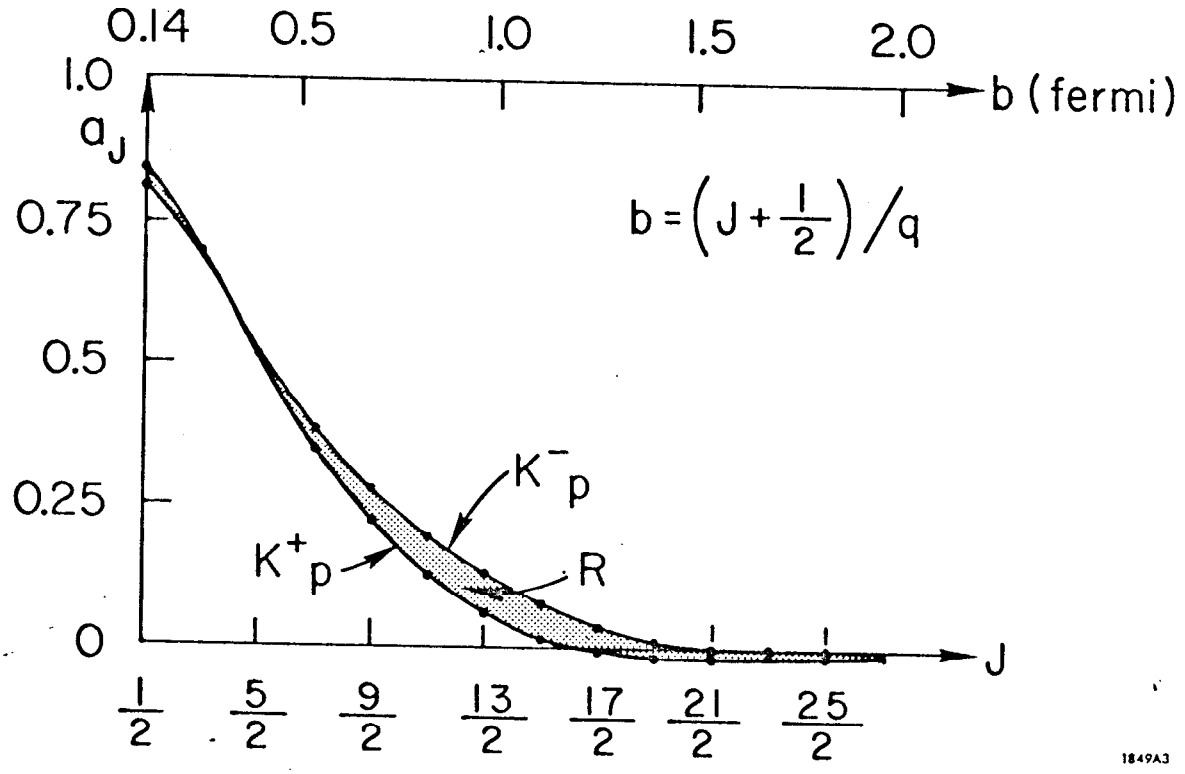
0.14
0.5
1.0
1.5
2.0
b (fermi)
1.0
a_J
0.75
0.5
0.25
0
$b = \left(J + \frac{1}{2}\right)/q$
K^-p
K^+p
R
J
$\frac{1}{2}$
$\frac{5}{2}$
$\frac{9}{2}$
$\frac{13}{2}$
$\frac{17}{2}$
$\frac{21}{2}$
$\frac{25}{2}$
1849A3

Fig. 3

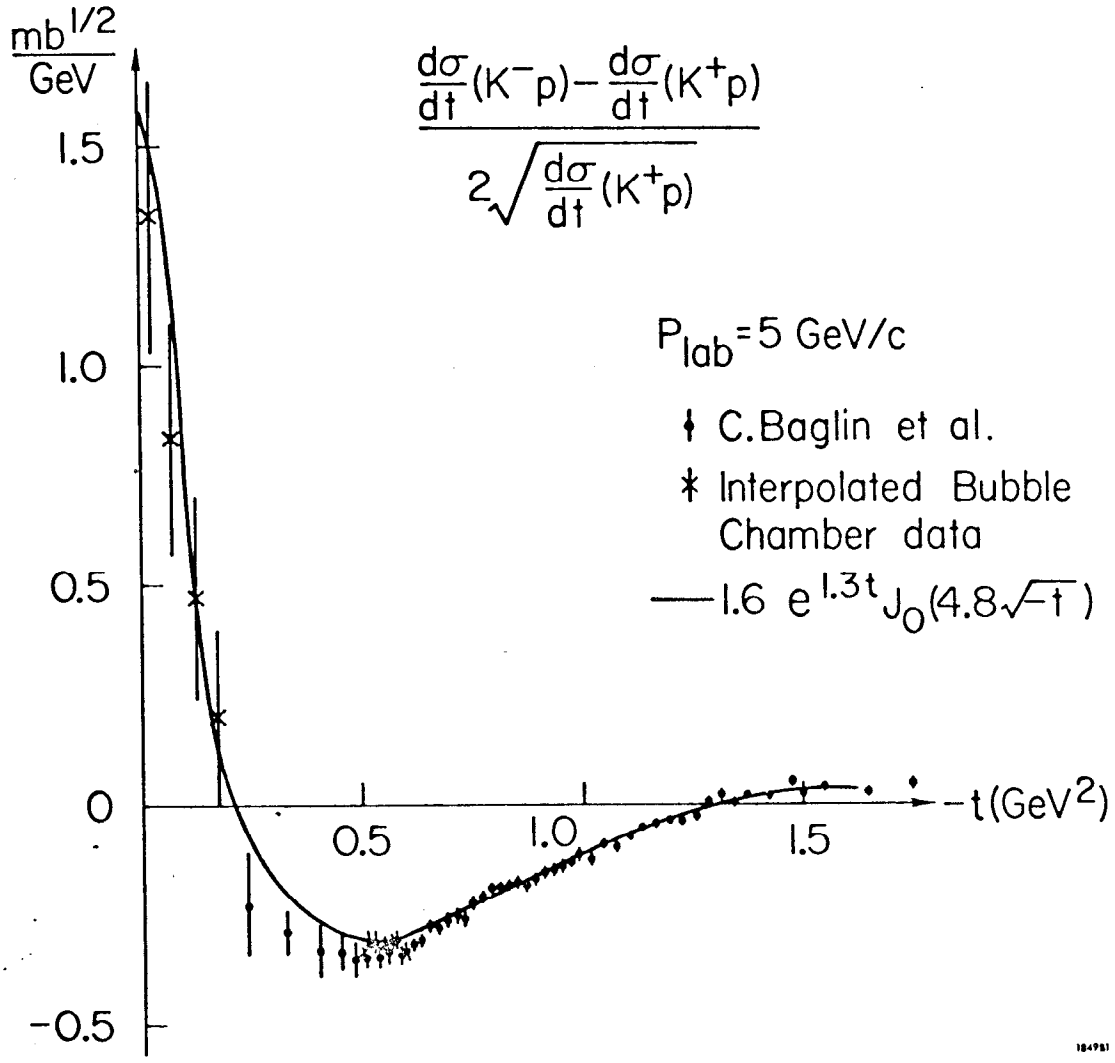
mb^1/2
GeV
1.5
1.0
0.5
0
-0.5
0.5
1.0
1.5
-t(GeV^2)
dσ/dt(K⁻p) − dσ/dt(K⁺p)
2√(dσ/dt(K⁺p))
P_lab = 5 GeV/c
C. Baglin et al.
Interpolated Bubble Chamber data
1.6 e^1.3t J_0(4.8√-t)

Fig. 4

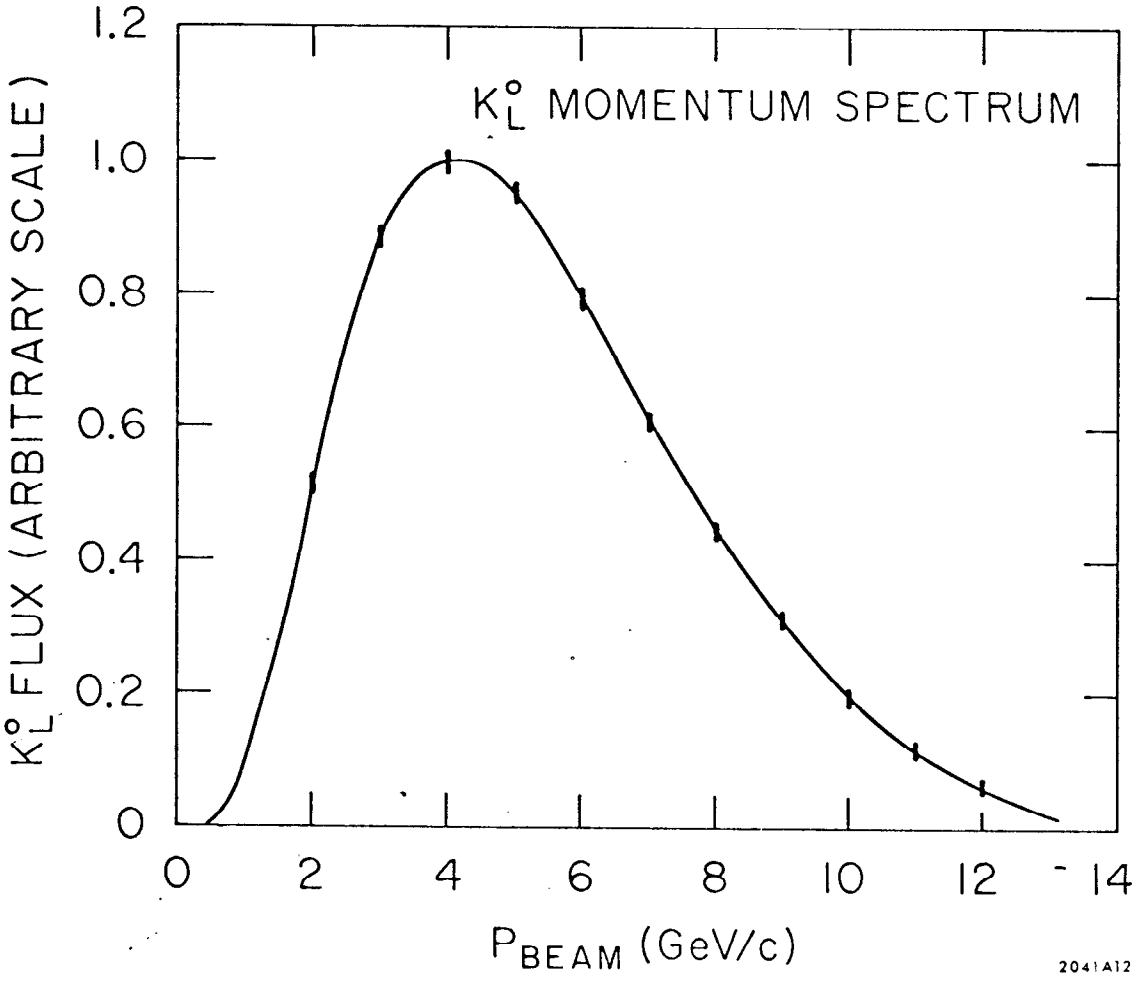
K_L° MOMENTUM SPECTRUM
K_L° FLUX (ARBITRARY SCALE)
1.2
1.0
0.8
0.6
0.4
0.2
0
0
2
4
6
8
10
12
14
P_{BEAM} (GeV/c)
2041A12

Fig. 5

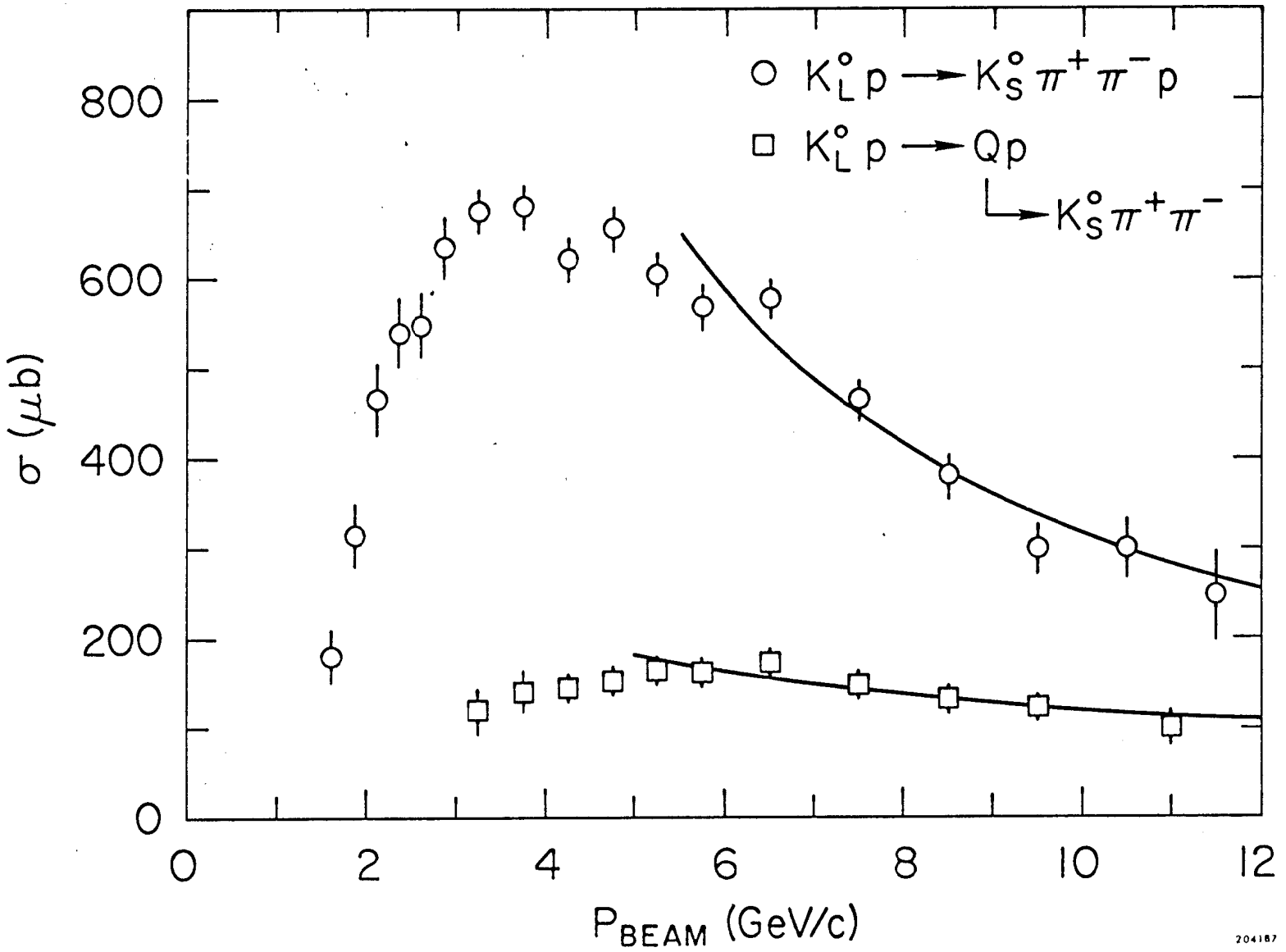
$K_L^0 p \rightarrow K_S^0 \pi^+ \pi^- p$
$K_L^0 p \rightarrow Qp$
$\hookrightarrow K_S^0 \pi^+ \pi^-$
σ (μb)
800
600
400
200
0
0
2
4
6
8
10
12
P_{BEAM} (GeV/c)
204187

Fig. 6

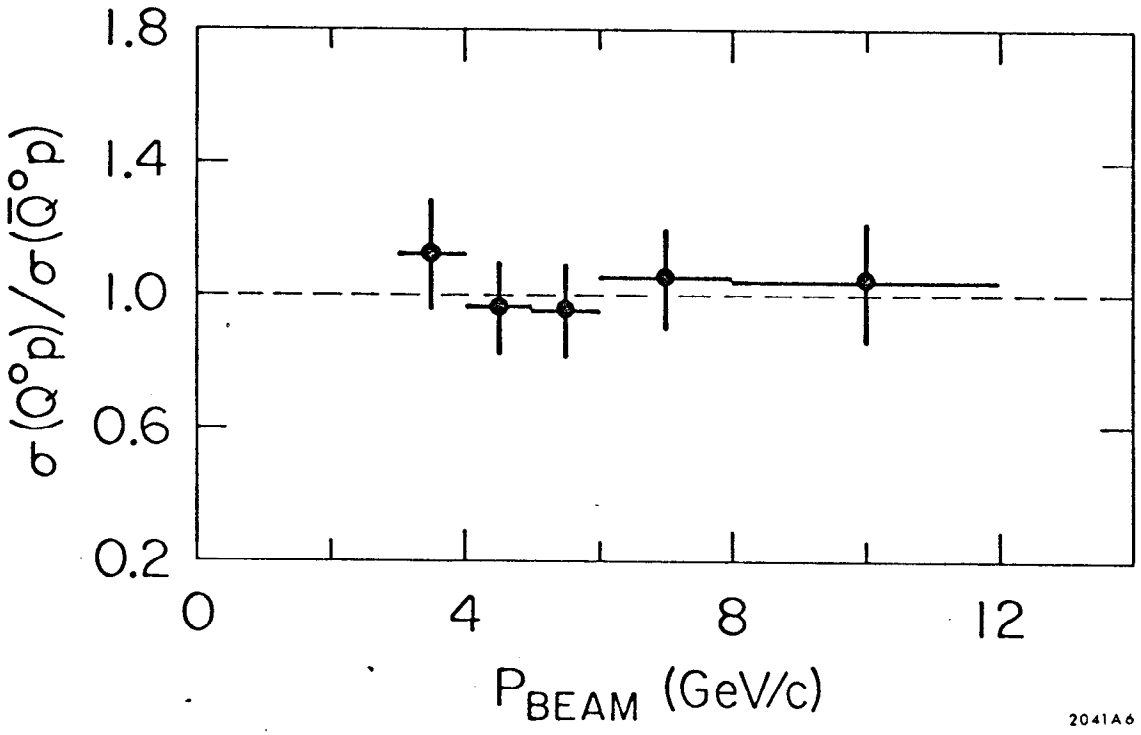

Fig. 7

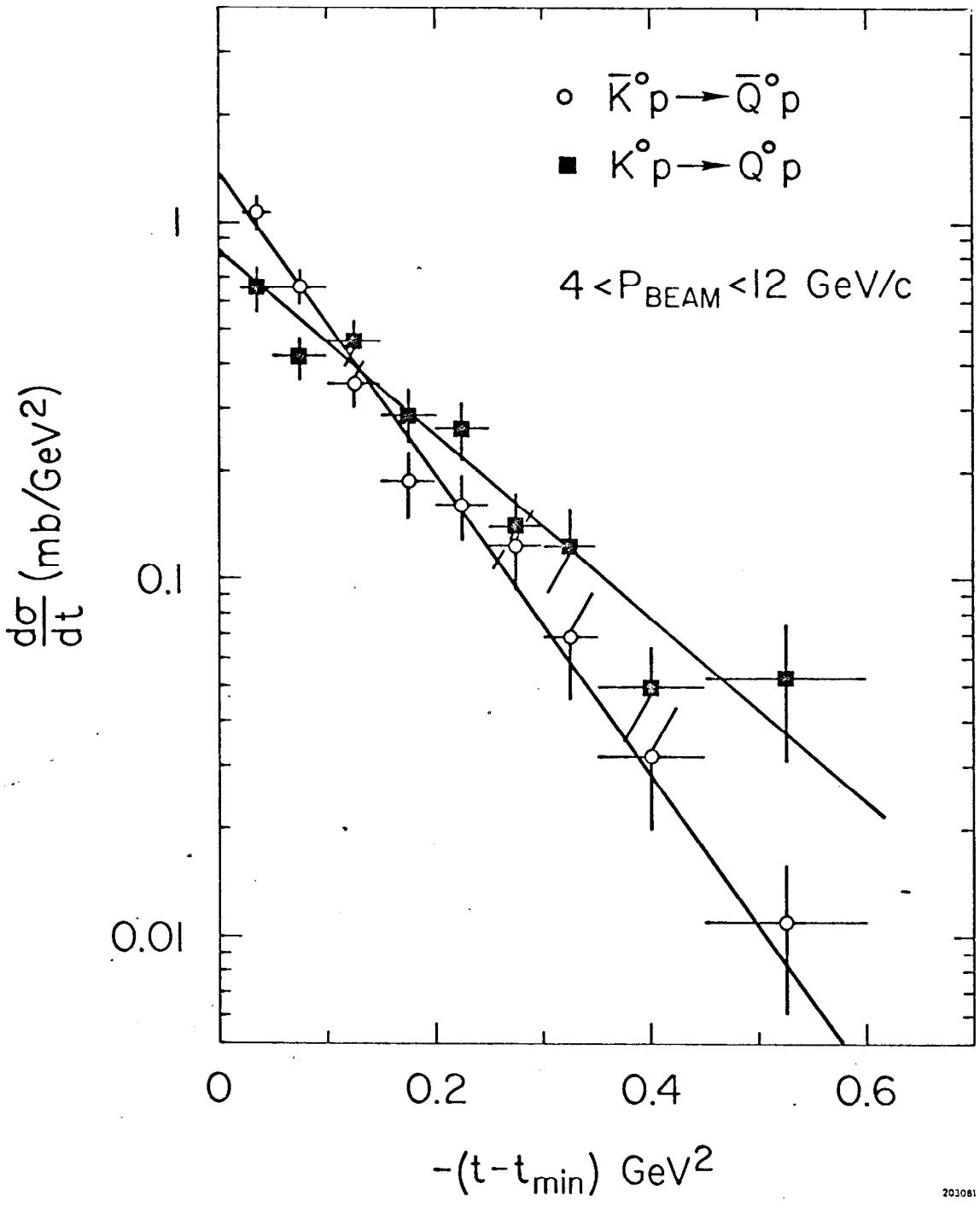
$\bar{K}^0p \rightarrow \bar{Q}^0p$
$K^0p \rightarrow Q^0p$
$4 < P_{BEAM} < 12$ GeV/c
$\frac{d\sigma}{dt}$ (mb/GeV^2)
1
0.1
0.01
0
0.2
0.4
0.6
$-(t-t_{min})$ GeV^2
203081

Fig. 8

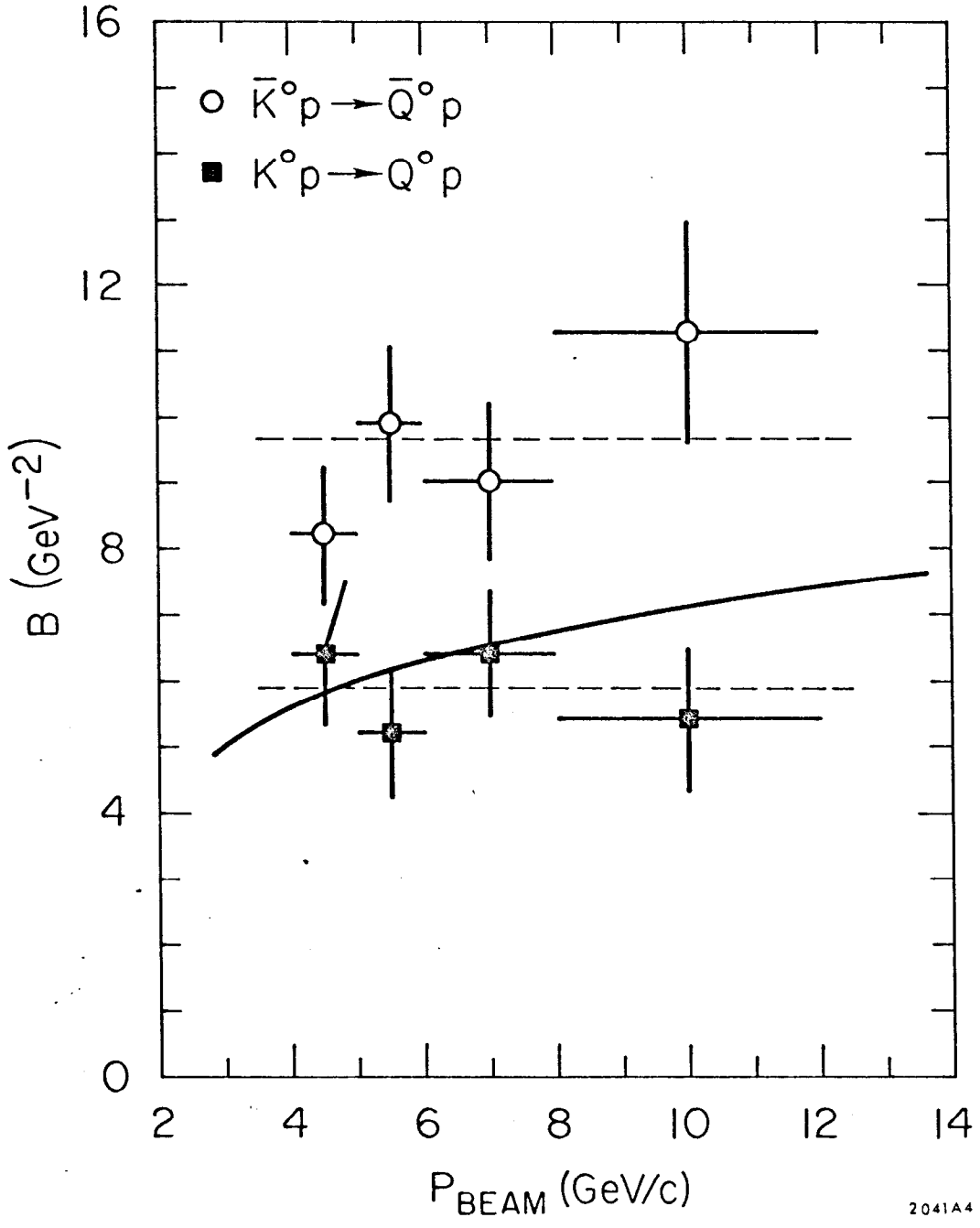
16
12
8
4
0
B (GeV^{-2})
$\bar{K}^0p \rightarrow \bar{Q}^0p$
$K^0p \rightarrow Q^0p$
2
4
6
8
10
12
14
P_{BEAM} (GeV/c)
2041A4

Fig. 9

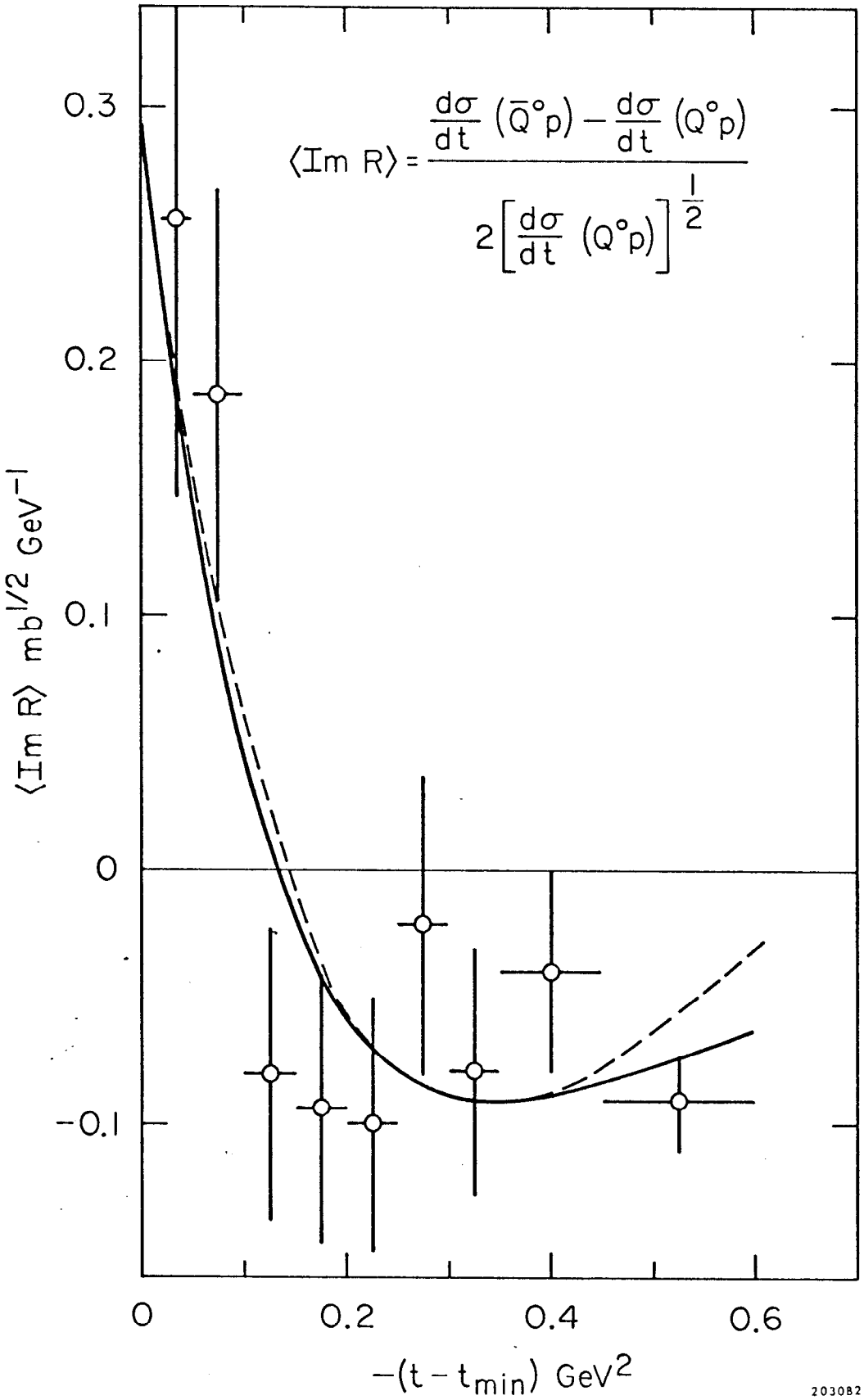
$\langle \text{Im } R \rangle = \dfrac{\frac{d\sigma}{dt}(\bar{Q}^\circ p) - \frac{d\sigma}{dt}(Q^\circ p)}{2\left[\frac{d\sigma}{dt}(Q^\circ p)\right]^{\frac{1}{2}}}$
0.3
0.2
0.1
0
-0.1
$\langle \text{Im } R \rangle$ mb$^{1/2}$ GeV^{-1}
0
0.2
0.4
0.6
$-(t - t_{min})$ GeV^2
203082

Fig. 10